

Original Article : Open Access

Exploring the anticancer potential of caffeic acid nanoemulsion: ROS induced apoptosis and cell cycle arrest in HCT116 colorectal cancer cells

Asad Ali*, Usama Ahmad*, Juber Akhtar*, Badruddeen**, Khursheed Ahmad***, Shivbrat Upadhyay***, Sahabjada Siddiqui***, Rumana Ahmad***, Puneet Khare****, Mohd Muazzam Khan** and Afroz Jahan*

* Department of Pharmaceutics, Faculty of Pharmacy, Integral University, Lucknow-226026, Uttar Pradesh, India

** Department of Pharmacology, Faculty of Pharmacy, Integral University, Lucknow-226026, Uttar Pradesh, India

*** Cell and Tissue Culture Lab, Era University, Lucknow-226003, Uttar Pradesh, India

**** CSIR-Indian Institute of Toxicology Research, Lucknow-226001, Uttar Pradesh, India

Article Info

Article history

Received 1 September 2023

Revised 17 October 2023

Accepted 18 October 2023

Published Online 30 December 2023

Keywords

Caffeic acid
Cancer
Drug delivery
Nanoemulsion
Phytoconstituent

Abstract

Caffeic acid, a prevalent phytoconstituent in plants, serves as a potent bioactive compound recognized for its robust antioxidant and anticancer properties. It is classified as a hydroxycinnamic acid and is renowned for its role in mitigating oxidative stress and inflammation. This attribute makes it an invaluable component in both natural remedies and biomedical research. This study presents an approach focused on the development and assessment of a caffeic acid loaded nanoemulsion (CALN), targeting its potential application in combating human colorectal cancer. The nanoformulation was achieved through an aqueous titration method, with Sefsol 218 (12% v/v) as the oil phase, Triton X100 as the surfactant, and propylene glycol as the co-surfactant (Smix; 2:1; 28% v/v). The aqueous phase comprised 60% v/v distilled water. Optimized nanoemulsion was rigorously evaluated using various parameters, including viscosity, particle size, zeta potential, polydispersity index, % transmittance, and refractive index. Notably, formulation E8 exhibited remarkable attributes, displaying a substantial drug release rate of 98.81% in 24 h, accompanied by a mean particle size of 40.08 nm, low polydispersity index of 0.17, zeta potential of -17.40 mV, viscosity of 21.40 cps, refractive index of 1.33, and percentage transmittance of 99.47. The stability analysis revealed that the formulated nanoemulsion retained its stability even under stress conditions. *In vitro* investigations unveiled the potential anticancer effects of the optimized caffeic acid loaded nanoemulsion against HCT 116 colorectal cancer cells. The nanoemulsion induced G2M phase arrest, induced alterations in cellular morphology, escalated ROS production, and demonstrated dose-dependent cytotoxicity in HCT 116 cells. These findings collectively highlight the promising role of caffeic acid loaded nanoemulsion as a potent oral delivery system for colorectal cancer.

1. Introduction

Caffeic acid stands out as a prominent phytoconstituent abundantly present in diverse plant sources, notably in coffee, various fruits, and vegetables. Within the plant kingdom, it serves a pivotal role as a robust antioxidant, safeguarding plants against oxidative stress and the harmful effects of UV radiation. Beyond its ecological significance, caffeic acid extends its influence on human health by offering substantial advantages. Its anti-inflammatory and anticancer attributes have aroused the interest of the medical community. This phytoconstituent's capacity to neutralize free radicals and mitigate oxidative harm, positions it as a valuable component in maintaining overall well-being through a balanced diet. Caffeic acid serves as a notable example of how plant compounds can offer both natural defense mechanisms and therapeutic potential for humans.

Natural products with anticancer properties have caught the interest of researchers because of their pharmacological and biological

functions (Dixit and Ali, 2010; Baker *et al.*, 2007; Prakash *et al.*, 2013). However, the toxic effects associated with chemotherapeutic agents remain a concerning issue. Polyphenolic compounds have a member called caffeic acid which is commonly present in coffee, olive oil, fruits, and vegetables (Liu *et al.*, 2013; Chang *et al.*, 2010; Kuo *et al.*, 2013; Ozturk *et al.*, 2012). Studies indicated the various physiological activities of caffeic acid and its derivatives like cardioprotective, antiproliferative, antiatherosclerotic, hepatoprotective, antihepatocellular carcinoma, anti-inflammatory, immunostimulatory, antiviral, antibacterial, antidiabetic, and antioxidant activity (Verma and Hansch, 2004; Silva *et al.*, 2014; Genaro-Mattos *et al.*, 2015; Tosovic, 2017; Lin and Yan, 2012; Rodrigues *et al.*, 2015; Kilani-Jaziri *et al.*, 2017; Agunloye *et al.*, 2019; Nagaoka *et al.*, 2002; Xie *et al.*, 2017; Yang *et al.*, 2013; Bispo *et al.*, 2017; Lee *et al.*, 2007; Won *et al.*, 2010; Gu *et al.*, 2016). Despite of enormous advantages of caffeic acid, studies revealed that caffeic acid has low oral bioavailability, low intestinal absorption, and poor permeability (Wang *et al.*, 2103). These shortcomings in caffeic acid put a barrier to providing maximum therapeutic action; therefore it is necessary to formulate caffeic acid into a form that can increase its bioavailability, intestinal absorption and permeability.

Nanostructured carrier systems have an edge over conventional delivery systems as they provide high bioavailability of active

Corresponding author: Dr. Usama Ahmad

Associate Professor, Department of Pharmaceutics, Faculty of Pharmacy, Integral University, Lucknow-226026, Uttar Pradesh, India

E-mail: usamaahmad.10@outlook.com

Tel.: +91-9554333085

Copyright © 2023 Ukaaz Publications. All rights reserved.

Email: ukaaz@yahoo.com; Website: www.ukaazpublications.com

pharmaceutical ingredients, specific tissue targeting and enhanced cellular interactions (Shi *et al.*, 2010). Utilizing nanostructured carrier systems can provide solutions to numerous challenges that are faced in the delivery of drugs (Wagner *et al.*, 2006). Nowadays nanostructures like nanoparticles are also used as a diagnostic tool (Imad Uddin *et al.*, 2020). Nanostructured drug delivery systems proved to be a more promising and potential system for the delivery of genetic biomolecules and compounds that have low aqueous solubility (Zhang *et al.*, 2008). The fabrication of nanostructured drug delivery systems aims at providing better bioavailability and encompasses the incorporation of therapeutically active substances into inactive lipid vehicles (Aungst, 1993) like oils (Burcham *et al.*, 1997), surfactants (Serajuddin *et al.*, 1988; Serajuddin, 1999; Aungst *et al.*, 1994), self-emulsifying formulations (Toguchi *et al.*, 1990; Wu *et al.*, 2006), emulsions (Kararli *et al.*, 1992; Myers and Stella, 1992; Palin *et al.*, 1986), micro or nanoemulsions (Lawrence and Rees, 2012; Akhtar *et al.*, 2016; Jadhav *et al.*, 2006), and liposomes (Schwendener and Schott, 1996). A set of advantages are associated with nanoemulsions over conventional drug delivery systems like quick onset of action, high kinetic and thermodynamic stability to prevent coalescence and aggregation (Saroja *et al.*, 2023) increased capacity for drug solubilization, longer shelf life (Shafiq-un-Nabi *et al.*, 2007), low toxicity, high lipid content, and production at large scale by methods like high-pressure homogenization (Mehnert and Mader, 2012).

This work focuses on the fabrication and optimization of stable nanoemulsion of caffeic acid by titration method (aqueous). The prepared CALN was further assessed based on PDI, refractive index, droplet size, zeta potential, viscosity, morphology, and release of drug in *in vitro* condition. Caffeic acid loaded nanoemulsion was also assessed against colorectal cancer cells.

2. Material and Methods

Caffeic acid was obtained as a gift sample from SD Fine Chem Ltd., Triton X-100 and propylene glycol were purchased from Sisco Research Laboratories and SD Fine Chem Ltd., respectively. Nikko Chemicals (Tokyo, Japan) sent a complimentary sample of Sefsol 218 and Sefsol 228.

The following items were bought from Himedia, India: MTT (3-(4,5-Dimethylthiazol-2-yl)-2,5-Diphenyltetrazolium Bromide) dye, FBS (foetal bovine serum), McCoy's 5A medium and antibiotic solution. DCFH-DA (2,7-dichlorodihydrofluorescein diacetate), PI (propidium iodide), and DAPI (4',6-Diamidino-2-phenylindole) dye were acquired from Sigma-Aldrich, USA. High purity grade reagents were utilized throughout.

NCCS, Pune, India, provided the HCT116 (human colorectal cancer) cell line. In addition to 10% (v/v) foetal bovine serum, 2.0 mM L-glutamine, 1.5 g/l NaHCO₃, 0.1 mM non-essential amino acids, and 1.0 mM sodium pyruvate, cell lines were cultured in McCoy's 5A medium. Cells were cultured in humidified air at 5% CO₂ and 37°C.

2.1 Development of nanoemulsion and its characterization

The solubility of caffeic acid in different oils was estimated, pseudoternary phase diagram was constructed and tests related to thermodynamic stability were performed to create a well-defined, robust, and stable nanoemulsion that was not affected by the change in temperature.

2.2 Oil phase screening using solubility studies

The solubility of caffeic acid in different oils was checked to find out which oil has the maximum potential for loading caffeic acid and this aspect of oil selection is crucial for the development of nanoemulsion. For this study, Sefsol 218, Sefsol 228, isopropyl myristate, and olive oil were selected. Vials of capacity 5 ml were taken and 2 ml of each oil was put into those vials. Moreover, an excess quantity of the drug (caffeic acid) was added and with the help of a vortex mechanical shaker the drug was dissolved (Shafiq *et al.*, 2007; Singh *et al.*, 2022). These vials were maintained in an isothermal shaker at 25 ± 1.0°C for 72 h to establish equilibrium. Following equilibrium, these vials were taken off from the shaker and centrifuged for 15 min at 10,000 revolutions per min. The supernatant (a transparent liquid) was collected and filtered using a membrane filter with a 0.45 µm pore size. The content of caffeic acid in various oils was also measured using a UV spectrophotometer operating at a wavelength of 327 nm.

2.3 Study of the pseudoternary phase diagram

The titration method (aqueous) was used to prepare the pseudoternary phase diagram using three components namely distilled water, oil, and S_{mix} (mixture of surfactant and co-surfactant) (Kommuru *et al.*, 2001). To get the best results, surfactant and co-surfactant were combined in various ratios of 1:0, 1:1, 1:2, 1:3, 2:1, and 3:1. A stock of 20 ml was made for each ratio. For every pseudoternary phase diagram, oil and S_{mix} were mixed in separate glass vials in different ratios from 1:9 to 9:1. Sixteen distinct combinations of oil and S_{mix} (1:9, 2:8, 3:7, 4:6, 5:5, 6:4, 7:3, 8:2, 9:1, 1:2, 1:3.5, 1:4, 1:5, 1:6, 1:7, 1:8) were titrated with distilled water and were examined for flow property and transparency (Lawrence and Rees, 2012). The pseudoternary phase diagram has three axes which represent the oil phase, the S_{mix} phase, and the aqueous phase. This diagram shows the physical condition of the produced nanoemulsion. The nanoemulsion area was displayed for each diagram, and the wider zone corresponds to higher self-nanoemulsifying efficiency. With the help of this diagram, distinct nanoemulsion were chosen from the nanoemulsion region of the phase diagram which had a minimum S_{mix} concentration and varying proportion of oil (10-30% v/v). Stability and dispersibility studies on a few selected nanoemulsions were performed further.

2.4 Thermodynamic stability tests

The following tests like centrifugation test, freeze-thaw cycle, and heating-cooling cycle were carried out on selected nanoemulsions.

Centrifugation test: The fabricated nanoemulsions were centrifuged for 30 min at 5000 revolutions per min while being visually checked for cracking, creaming, or separation of layers.

Freeze-thaw cycle: In this cycle, the effect of keeping the nanoemulsion at -20°C and 20°C was examined. The nanoemulsions were kept for a minimum period of 24 h at -20°C as well as at 20°C.

Heating-cooling cycle: In this cycle, the effect of storing the chosen nanoemulsion at 45°C and 0°C was investigated. The nanoemulsions were kept for a minimum period of 48 h at 45°C as well as at 0°C.

Three cycles of the above-mentioned thermodynamic stability stress test were performed for every group of nanoemulsion to get more authentic results for the accelerated stability test. To further study these nanoemulsions, we selected those nanoemulsions that demonstrated the best stability (Akhtar, 2015).

2.5 Evaluations of dispersibility

The ability of emulsification on its own of the prepared nanoemulsion was examined in type II USP dissolution apparatus at $37 \pm 0.5^\circ\text{C}$ by adding 1 ml of nanoemulsion in 0.5 liters of 0.1N

hydrochloric acid and distilled water. To apply gentle agitation, a paddle made up of stainless steel was rotated at 75 rotations per min in the type II USP dissolution apparatus. Nanoemulsions were inspected visually and grades were assigned to the nanoemulsion according to Table 1.

Table 1: Visual inspection of nanoemulsion

S. No.	Grade	Comments	Formation time	Appearance
1	A	Clear and transparent nanoemulsion	Rapid (within 1 min)	Bluish tint
2	B	Slightly less clear and low transparency than Grade A	Rapid (within 1 min)	Bluish white tint
3	C	Emulsion with a fine milky appearance	Established within 2 min	White tint
4	D	The emulsion has a slightly oily and dull white look	Steady (more than 2 min)	Dull grayish-white tint
5	E	Globules of oil present on the surface of the formulation due to poor or minimal emulsification	Slow (longer than 2 min)	Dull grayish-white tint

The nanoemulsions that qualifies thermodynamic stability test and falls under Grade A and Grade B of the dispersibility test were selected for preparing the nanoemulsion with the drug (caffeic acid).

2.6 Fabrication of caffeic acid loaded nanoemulsion (CALN) by titration method (aqueous)

Titration method (aqueous) was employed to formulate caffeic acid loaded nanoemulsion (CALN), keeping the water as the continuous phase. According to the pseudoternary phase diagram, the region where the concentration of the oil phase should be such that, it is capable of dissolving the highest amount of caffeic acid was used to prepare CALN and these formulations were used for the final investigations. To create distinct caffeic acid loaded nanoemulsions, different amounts of sefsol 218 were chosen from the established phase diagrams that solubilized the highest amount of caffeic acid. Moreover, from the ternary phase diagrams only those nanoemulsions were selected that had the minimum concentration of surfactant. While the pseudoternary phase diagram's emulsifying areas served as the basis for choosing the S_{mix} ratios, oil, and aqueous medium for the fabrication of CALN. In the end, sefsol 218 was chosen as the oil, triton X100 as the surfactant, and propylene glycol as the co-surfactant. The sample was then diluted by adding water drop by drop while being continuously vortexed, until it was transparent and clear, with or without a tint of blue colour.

2.7 Physicochemical analysis and assessment of CALN

2.7.1 Assessment through visual examination

To differentiate between CALN and microemulsion visual observation was done.

2.7.2 Quantification utilizing DLS (dynamic light scattering)

This was used to determine the average droplet size and polydispersity index (PDI) of CALN using a zetasizer. Due to the Brownian motion of the particle, the light is scattered which is detected by the zetasizer at 90° angle and 25°C . Distilled water was added to the sample to make them less concentrated and then passed through a membrane filter having a pore size of $0.45 \mu\text{m}$, and finally placed into the module (Akhtar, 2015; Imad Uddin and Veeresh, 2020).

2.7.3 Viscosity determination

Viscosity of CALN was examined at $25 \pm 0.5^\circ\text{C}$ using a Brookfield viscometer attached with spindle number 40 (DV III ultra V6.0 RV cone and plate rheometer).

2.7.4 Refractive index and percent transmittance

By placing a drop of CALN on the slide of the Abbe refractometer at 25°C the refractive index of CALN was determined. Using a UV spectrophotometer at 327 nm, the per cent transmittance of CALN was measured (Parveen *et al.*, 2010).

2.7.5 Transmission electron microscopy (TEM)

TEM TOPCON 002B (Topcon, Oakland, NJ) was adopted to examine the structure of the surface of CALN (Parveen *et al.*, 2010). Distilled water was used to dilute the sample of CALN in the ratio (1:100), and then by using a membrane filter of pore size $0.22 \mu\text{m}$ the CLAN was filtered and applied on a carbon-coated grid with 2% phosphotungstic acid and left for 30 seconds. On a slide, the dried coated grid was placed and a cover slip was placed over it. A light microscope operating at 200 KV was used to examine the slide (Deka *et al.*, 2021).

2.7.6 In vitro drug release study

Utilizing USP type II dissolution equipment, the drug release experiment was carried out in simulated intestinal fluid (900 ml) at 50 rotations per minute and $37 \pm 0.5^\circ\text{C}$. The treated dialysis bag (molecular weight cut-off 1200 g/mole) was filled with 1 ml of a CALN formulation. At constant time intervals (0, 0.5, 1, 1.5, 2, 2.5, 3, 4, 6, 8, 12, 20, and 24 h) 1 ml of the sample was taken out and was substituted with the equal quantity of simulated intestinal fluid (Akhtar *et al.*, 2014). Using a UV spectrophotometer set to 327 nm, the samples were examined for drug content. Comparisons between the release of the drug from nanoemulsion formulations and traditional suspension were made.

2.7.7 Stability studies

Accelerated stability test was performed on the optimized CALN at $40 \pm 2^\circ\text{C}/75 \pm 5\% \text{RH}$ for 6 months. CALN was kept in glass bottles inside the stability chamber (Thermolab, Mumbai, India) where the temperature and humidity were controlled. At predetermined intervals of 0, 90, and 180 days, measurements were made in terms of PDI, zeta potential, refractive index, droplet size, viscosity, and % transmittance (Akhtar *et al.*, 2014).

2.8 *In vitro* anticancer study

2.8.1 Assessment of cellular cytotoxicity through the MTT assay

The enzymatic reduction of the MTT dye provides the basis for this test. MTT test was carried out in accordance with a prior procedure to assess the antiproliferative impact of caffeic acid loaded nanoemulsion (Jigyasu *et al.*, 2020). HCT116 cells (1×10^4) were added in each well of a 96-well culture plate containing 100 μ l of complete media and left overnight at 5% CO₂ and 37°C. To achieve the appropriate concentrations (10, 25, 50, and 100 μ g/ml), stock solutions of CALN were made in placebo and diluted in culture medium. Now as per the experimental design, this solution was added to the wells. 10 μ l of the MTT (5 mg/ml stock solution in PBS) solution was added to each well after the 24 h treatment time, and the plate was then incubated at 37°C for an additional 3 h to allow a formazan blue crystal to form. Then, after removing the supernatant from each well, the formazan crystals were dissolved in 100 μ l of DMSO at 37°C for 10 min. The proportion of live cells was ascertained by measuring the absorbance at 540 nm with a microplate reader (BIORAD-PW41, California, USA). The Japanese Nikon ECLIPSE TS100 inverted phase contrast microscope was adopted to investigate alterations in cellular structure.

2.8.2 DAPI staining to assess the impact of CALN on the chromatin condensation in HCT116 cells

Following a previous technique, the apoptotic impact of CALN at two effective doses (40 and 75 ng/ml) was examined (Ahmad *et al.*, 2018). In a 96-well plate, the cells were introduced and then kept for 24 h. A 4% solution of paraformaldehyde was used to fix the cells for 10 min after the suggested 24 h time period had passed and phosphate buffer solution was used to wash the cells. The cells were then permeabilized using permeabilization buffer, which contains Triton X-100 (0.5%) and paraformaldehyde (3%), and finally, DAPI staining was performed. The photos were captured using a fluorescence microscope after the DAPI staining.

2.8.3 Reactive oxygen species (ROS) activity

According to the previous publication, the amount of reactive oxygen species within cells was measured using flow cytometry by employing the DCFH-DA dye (Jafri *et al.*, 2019). Two effective doses of CALN (40 and 75 ng/ml) were applied to HCT116 cells (2×10^5 per well),

which had been placed in a 6-well culture plate overnight. The CALN treatment was continued for 12 h. To measure the intensity of ROS both untreated and treated cells were harvested and phosphate buffer solution was used to wash it and incubated in phosphate buffer solution containing 10 μ M DCFH-DA dye at 37°C for 20 min. After that phosphate buffer solution was used to wash the cell and the washing was done twice. Lastly, cells were analysed using a flow cytometer (BD FACSLytic Flow Cytometer, USA).

2.8.4 Analysis of cell cycle phases

The distribution of cell cycle stages and the degree of concentration of cellular DNA were determined using flow cytometry by adopting a previously described approach (Siddiqui *et al.*, 2014). 2×10^5 cells/ml of HCT116 cells were seeded into 6-well plates and left overnight. After that, the cells were exposed to 40 and 75 ng/ml of caffeic acid loaded nanoemulsion for 24 h. Cold phosphate buffer solution was used to wash the cultured cell and with the help of ethanol (70%) the cells were fixed at -20°C for 2 h. Propidium iodide was used for staining cells that had been fixed for 30 min at room temperature after RNase A (10 mg/ml) treatment. A flow cytometer (BD FACSLytic Flow Cytometer, USA) was used to quantify the propidium iodide fluorescence in each nucleus. Cell Quest Pro V 3.2.1 software (Becton Dickinson, USA) was used to analyze the data.

2.8.5 Statistical analysis

The findings of cell viability were reported as the mean \pm standard deviation of three separate studies. For significance testing, one-way ANOVA was used with $p \leq 0.05$.

3. Results

3.1 Solubility studies

Finding an optimal oil phase for the production of CALN that would produce the maximum potential for the loading of the drug was the aim of the solubility investigation. The drug must have high oil phase solubility so that the developed nanoemulsion can retain the drug in the solubilized state. Caffeic acid showed maximum solubility in sefsol 218 (20 mg/ml), followed by sefsol 228 (16.5 mg/ml), isopropyl myristate (13.6 mg/ml), and olive oil (11.2 mg/ml). The results obtained during experiments are depicted in Figure 1.

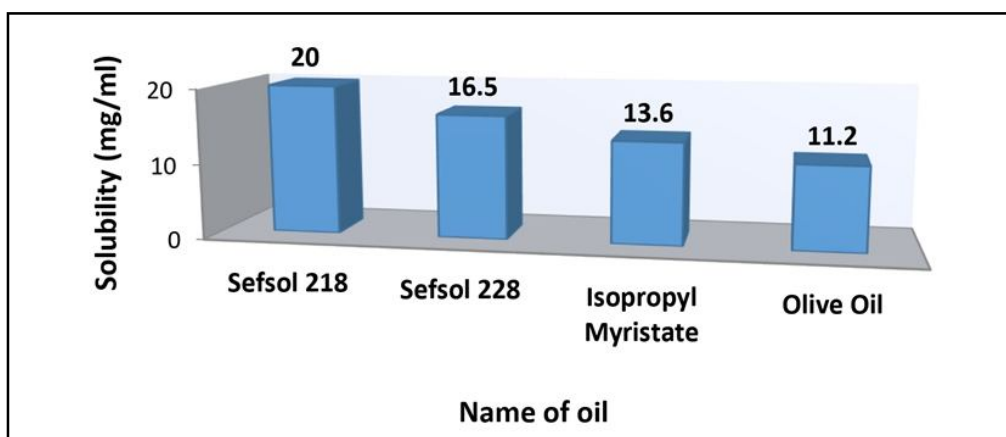


Figure 1: Solubility of caffeic acid in different oils.

Among the surfactants, PEG 400 has the highest potential to solubilize caffeic acid (66.8 mg/ml), followed by triton X100 (50.2 mg/ml),

propylene glycol (45.7 mg/ml) and kolliphor RH 40 (26.4 mg/ml). The results obtained during this study are depicted in Figure 2.

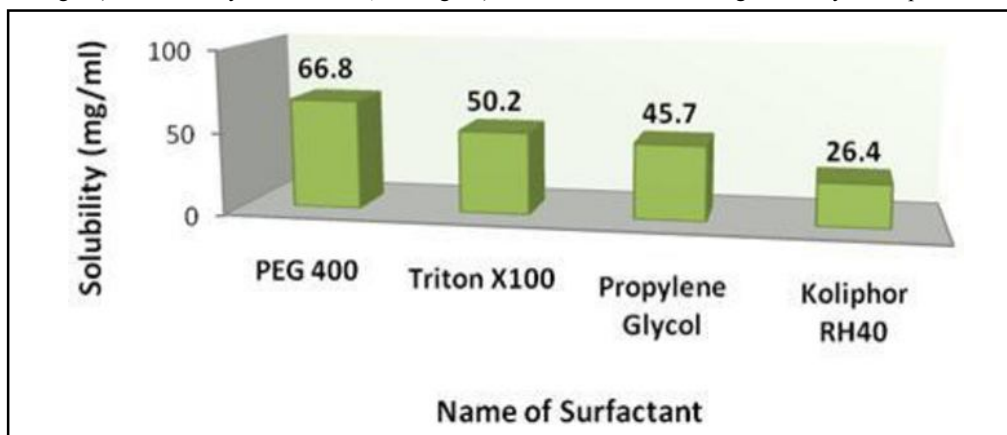


Figure 2: Solubility of caffeic acid in different surfactants.

Caffeic acid was maximum soluble in PEG 400; however, it was not selected for formulating nanoemulsion because the nanoemulsion obtained by utilizing PEG 400 as surfactant gave turbid nanoemulsion

whereas the nanoemulsion obtained by using triton X100 as surfactant provided clear transparent nanoemulsion with bluish tint, hence triton X100 was selected as a surfactant for further study.

3.2 Study of the pseudoternary phase diagram

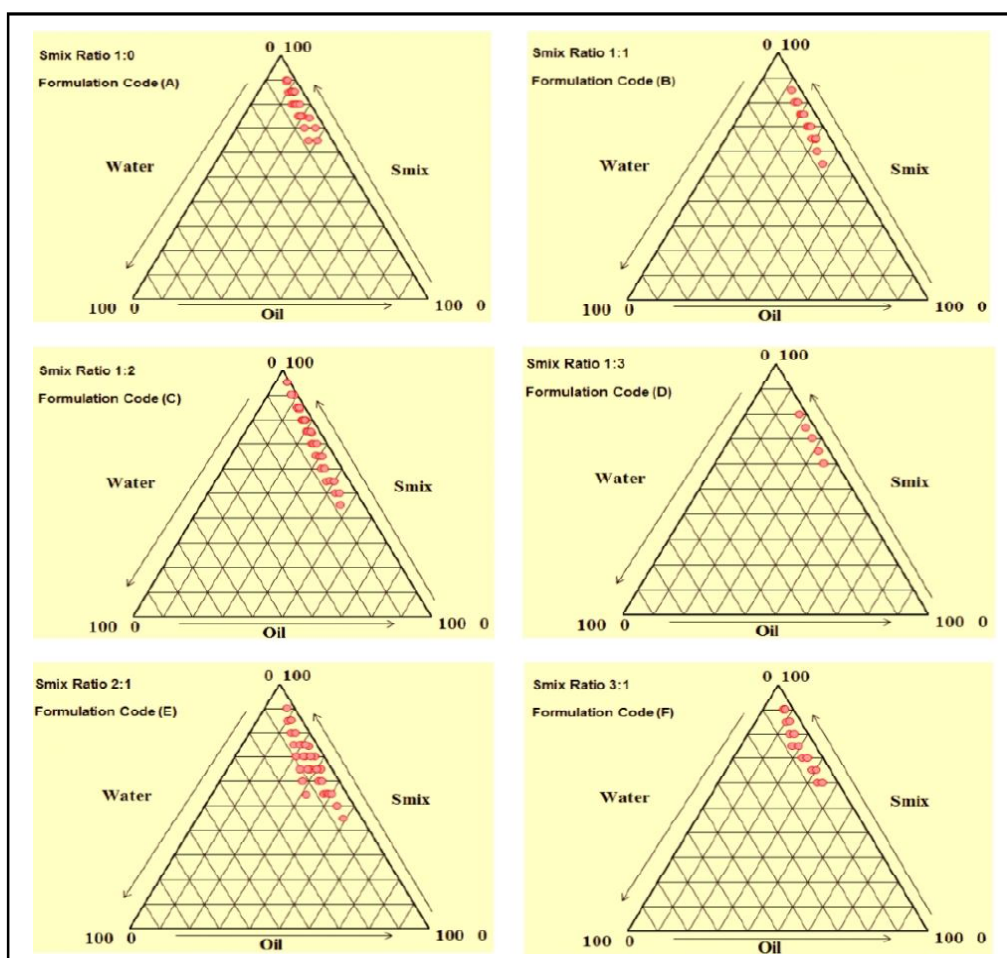


Figure 3: Pseudoternary phase diagrams of formulated nanoemulsions, A (S_{mix} 1:0), B (S_{mix} 1:1), C (S_{mix} 1:2), D (S_{mix} 1:3), E (S_{mix} 2:1) and F (S_{mix} 3:1).

Sefsol 218 was used as the oil phase and triton X100 was used as the surfactant in a phase diagram of nanoemulsion, which demonstrated that the small amount of oil could be dissolved at greater surfactant concentrations (Figure 3A). It produced a limited range for the formation of nanoemulsions. A co-surfactant or amphiphilic molecule is often needed to lower the surface tension of the oil to virtually zero because a surfactant alone is typically insufficient to considerably reduce the oil's interfacial tension to form a nanoemulsion. To add fluidity to the interfacial film and disperse the liquid crystalline phases that are produced when the surfactant film becomes too rigid, co-surfactants penetrate the surfactant monolayer. This can be clarified through the simple fact that a solo surfactant is seldom able to form an interfacial film between the fluid; normally, a co-surfactant is also needed. Nanoemulsion that contained co-surfactant as propylene glycol, surfactant as triton X100 and oil phase as sefsol 218 showed a broader area for the formation of nanoemulsion (Figures 3B and 3C) when compared to Figure 3A that only has surfactant and no co-surfactant. Moreover, among B (S_{mix} 1:1) and C (S_{mix} 1:2), C showed the formation of broader nanoemulsion regions suggesting that increasing the concentration of co-surfactant increases the chance of development of nanoemulsion which were transparent in appearance with a slight blue tint. Additionally, a surfactant and co-surfactant combination in the ideal concentration results in a significant amount of oil phase solubilization. Propylene glycol, a co-surfactant, lowers the interface's bending stress and renders the

interfacial layer sufficiently malleable to adopt the several curvatures needed to develop nanoemulsions throughout a range of compositions. The maximum concentration of co-surfactant which could be added in the S_{mix} is in the ratio 1:2 because as we increase the concentration of co-surfactant in a S_{mix} like 1:3 there is a decrease in the formation of nanoemulsion region which can be clearly seen in Figure 3D. The maximum concentration of surfactant which could be added in the S_{mix} is in the ratio 2:1 because as we decrease the concentration of surfactant from 2 to 1 or increase it from 2 to 3, the area of formation of nanoemulsion also decreases which is depicted by Figure 3C and Figure 3F, respectively. As a result, crucial information regarding the role and quantity of aqueous phase, co-surfactants, and surfactants in the formulation of nanoemulsions is provided by the pseudoternary phase diagram analysis (Figure 3). The phase diagrams showed that S_{mix} ratio of 2:1 provided better results when compared with other S_{mix} ratio.

3.3 Examination of thermodynamic stability

The formulated nanoemulsion was put through stability experiments after the nanoemulsion region had been optimized. Most of the nanoemulsions continued to be stable under stressful circumstances. Three tests, the freeze-thaw cycle, heating/cooling cycle, and centrifugation were conducted to evaluate the stability of the nanoemulsion. Table 2 is a list of the findings observed during the testing.

Table 2: Examination of thermodynamic stability of prepared nanoemulsion

Code	Ratio of S_{mix}	Oil %	S_{mix} %	Water%	Thermodynamic stability test			Dispersibility		Result
					Centrifugation	Freeze-thaw cycle	Heating-cooling cycle	0.1 N HCl	H ₂ O	
A1	1:0	2.99	26.87	70.15	P	P	P	A	A	P
A2		3.00	23.00	75.00	P	P	P	C	C	F
A3		5.00	20.00	75.00	P	P	P	A	A	P
A4		4.00	16.00	80.00	P	P	P	A	A	P
A5		3.08	12.31	84.62	F	-	-	-	-	F
A6		6.00	14.00	80.00	P	P	P	C	C	F
A7		4.62	10.77	84.62	P	P	P	C	C	F
A8		3.00	7.00	90.00	P	P	P	B	B	F
A9		6.25	18.75	75.00	F	-	-	-	-	F
A10		5.00	15.00	80.00	P	F	-	-	-	F
A11		3.74	11.21	85.05	F	-	-	-	-	F
A12		3.00	8.00	90.00	F	-	-	-	-	F
A13		7.75	27.13	65.12	P	P	F	-	-	F
A14		6.67	23.33	70.00	P	P	P	A	A	P
A15		5.56	19.44	75.00	F	-	-	-	-	F
A16		4.44	15.56	80.00	F	-	-	-	-	F
A17		3.33	11.67	85.00	F	-	-	-	-	F
A18		2.22	7.78	90.00	F	-	-	-	-	F
A19		3.33	16.67	80.00	F	-	-	-	-	F

A20		2.50	12.50	85.00	F	-	-	-	-	F
A21		5.00	30.00	65.00	P	P	P	C	C	F
B1	1:1	5.00	20.00	75.00	P	P	P	A	A	P
B2		4.00	16.00	80.00	P	P	P	A	A	P
B3		3.08	12.31	84.62	F	-	-	-	-	F
B4		7.49	37.45	55.06	P	P	P	C	C	F
B5		6.67	33.33	60.00	P	P	P	B	B	F
B6		5.80	28.99	65.22	P	F	-	-	-	F
B7		5.00	25.00	70.00	P	F	-	-	-	F
B8		4.17	20.83	75.00	P	F	-	-	-	F
B9		3.33	16.67	80.00	P	F	-	-	-	F
B10		5.00	30.00	65.00	F	-	-	-	-	F
B11		4.26	25.53	70.21	F	-	-	-	-	F
B12		3.57	21.43	75.00	F	-	-	-	-	F
B13		4.35	30.43	65.22	F	-	-	-	-	F
B14		3.74	26.17	70.09	F	-	-	-	-	F
C15	1:2	7.84	47.06	45.10	P	P	P	A	A	P
C23		5.56	44.44	50.00	P	P	P	A	A	P
C24		5.00	40.00	55.00	P	P	P	C	C	F
C25		3.88	31.07	65.05	P	P	F	-	-	F
C26		3.33	26.67	70.00	P	P	P	C	C	F
C27		2.78	22.22	75.00	P	P	P	C	C	F
D1	1:3	4.00	36.00	60.00	F	-	-	-	-	F
D2		3.51	31.58	64.91	F	-	-	-	-	F
D3		2.99	26.87	70.15	F	-	-	-	-	F
D4		3.00	23.00	75.00	P	P	P	C	C	F
D5		2.00	18.00	80.00	P	P	P	B	B	F
E1	2:1	3.51	31.58	64.91	P	P	P	B	B	F
E2		2.99	26.87	70.15	P	P	P	B	B	F
E3		3.00	23.00	75.00	P	P	P	B	B	F
E4		7.02	28.07	64.91	P	P	P	B	B	F
E5		5.97	23.88	70.15	P	P	P	A	A	P
E6		5.00	20.00	75.00	P	P	P	B	B	F
E7		13.64	31.82	54.55	P	P	P	B	B	F
E8		12.00	28.00	60.00	P	P	P	A	A	P
E9		10.53	24.56	64.91	F	-	-	-	-	F
E10		8.96	20.90	70.15	F	-	-	-	-	F
E11		7.50	17.50	75.00	F	-	-	-	-	F
E12		6.00	14.00	80.00	F	-	-	-	-	F
E13		4.62	10.77	84.62	F	-	-	-	-	F
E14		7.75	27.13	65.12	P	P	P	A	A	P
E15		6.67	23.33	70.00	F	-	-	-	-	F

E16		5.56	19.44	75.00	P	P	P	A	A	P
E17		4.44	15.56	80.00	F	-	-	-	-	F
E18		3.33	11.67	85.00	F	-	-	-	-	F
E19		2.22	7.78	90.00	F	-	-	-	-	F
E20		7.49	37.45	55.06	P	P	P	C	C	F
E21		6.67	33.33	60.00	P	P	P	C	C	F
E22		6.41	38.46	55.13	P	P	P	B	B	F
E23		5.71	34.29	60.00	P	P	P	B	B	F
E24		5.00	30.00	65.00	F	-	-	-	-	F
E25		4.26	25.53	70.21	F	-	-	-	-	F
E26		3.57	21.43	75.00	F	-	-	-	-	F
E27		5.62	39.33	55.06	P	P	P	A	A	P
E28		6.12	48.93	44.95	P	P	P	A	A	P
E29		5.56	44.44	50.00	P	P	P	A	A	P
E30		5.00	40.00	55.00	P	P	P	B	B	F
F1	3:1	7.50	17.50	75.00	P	F	-	-	-	F
F2		6.00	14.00	80.00	P	P	P	C	C	F
F3		4.62	10.77	84.62	P	F	-	-	-	F
F4		3.00	7.00	90.00	F	-	-	-	-	F
F5		6.67	23.33	70.00	P	P	P	C	C	F
F6		5.56	19.44	75.00	F	-	-	-	-	F
F7		4.44	15.56	80.00	P	P	P	A	A	P
F8		3.33	11.67	85.00	F	-	-	-	-	F
F9		2.22	7.78	90.00	F	-	-	-	-	F
F10		6.67	33.33	60.00	P	P	P	A	A	P
F11		5.80	28.99	65.22	P	P	P	C	C	F
F12		5.00	25.00	70.00	F	-	-	-	-	F
F13		5.00	35.00	60.00	P	P	P	B	B	F
F14		4.35	30.43	65.22	P	P	P	B	B	F

P = Pass, F = Fail

Table 3: Droplet size, PDI, zeta potential, refractive index, viscosity, and % transmittance of CALN with formulation code B1, E5 and E8

Code	Size of droplet (nm)	PDI	Zeta potential (mV)	Viscosity (cP)	Refractive index	Percentage transmittance
B1	29.82 ± 0.21	0.35 ± 0.007	-3.69 ± 0.19	19.84 ± 0.28	1.33 ± 0.005	99.26 ± 0.25
E5	43.61 ± 0.28	0.22 ± 0.01	-9.56 ± 0.21	18.67 ± 0.10	1.34 ± 0.01	99.35 ± 0.46
E8	40.08 ± 0.45	0.17 ± 0.01	-17.40 ± 0.35	21.40 ± 0.42	1.33 ± 0.01	99.47 ± 0.17

Every data point is presented as mean ± standard deviation (n = 3).

3.4 Fabrication of CALN

To make CALN, caffeic acid was added to that optimized nanoemulsion that passed every thermodynamic stability test and had the highest oil content.

3.5 Characterization and evaluation of nanoemulsion

The following parameters were used to characterize and evaluate the selected CALN formulations.

3.5.1 Visual appearance

The formulated CALN had no turbidity and was transparent and clear. A visual evaluation was used to detect macroemulsion, which has a milky look, in contrast to nanoemulsion which is clear with or without blue tint.

3.5.2 Dynamic light scattering (DLS) measurement

The droplet size, zeta potential, and polydispersity index were identified using the DLS approach (Figures 4A and 4B). Formulation

B1 showed the smallest droplet size of $(29.82 \pm 0.21 \text{ nm})$ followed by E8 ($40.08 \pm 0.45 \text{ nm}$) and E5 ($43.61 \pm 0.28 \text{ nm}$). Polydispersity index of formulation B1, E5, E8 were found to be 0.35 ± 0.007 , 0.22 ± 0.01 , 0.17 ± 0.01 , respectively. Results obtained in zeta potential, viscosity, refractive index, and percentage transmittance study are described in Table 3.

The lower value of PDI implies that the droplet sizes in the nanoformulations were uniform. The chosen ratio of aqueous phase, oil, co-surfactant, and surfactant was able to produce small, consistent droplets at nanosized scale. The findings, therefore, suggested that choosing the right ratio of S_{mix} , oil, and water was essential for fabricating a formulation that has a lower droplet size and is stable for a longer period of time.

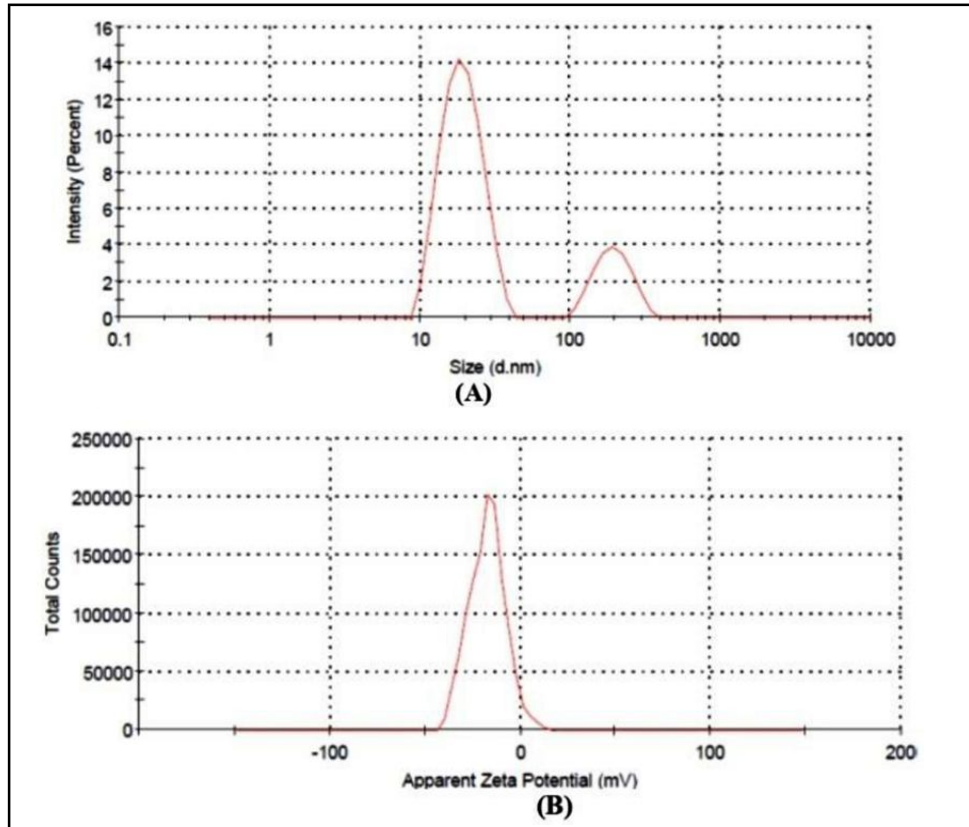


Figure 4: Caffeic acid loaded nanoemulsion, (A) represents droplet size and (B) zeta potential.

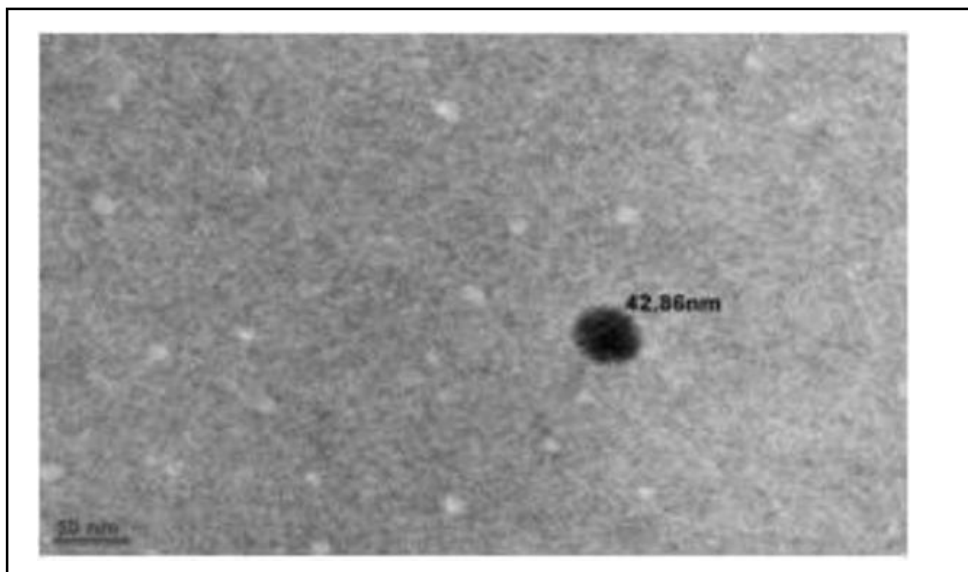


Figure 5: CALN seen under transmission electron microscope.

3.5.3 Transmission electron microscopy (TEM)

The TEM image of formulation E8 revealed that CALN had a droplet size of less than 50 nm (Figure 5).

3.5.4 *In vitro* drug release study

The optimized nanoformulations namely B1, E5, and E8 were compared with the prepared conventional suspension. By

extrapolating the calibration curve, the concentration was determined, and a graph between the release of the drug in percentage and time was plotted (Figure 6). The nanoformulation E8 showed a much better drug release profile of 98.81% 3 times more in 24 h than the prepared conventional suspension which only had a drug release of 31.09% in the same time. The nanoformulation E5 and B1 showed drug release of 94.21% and 84.07% respectively in 24 h.

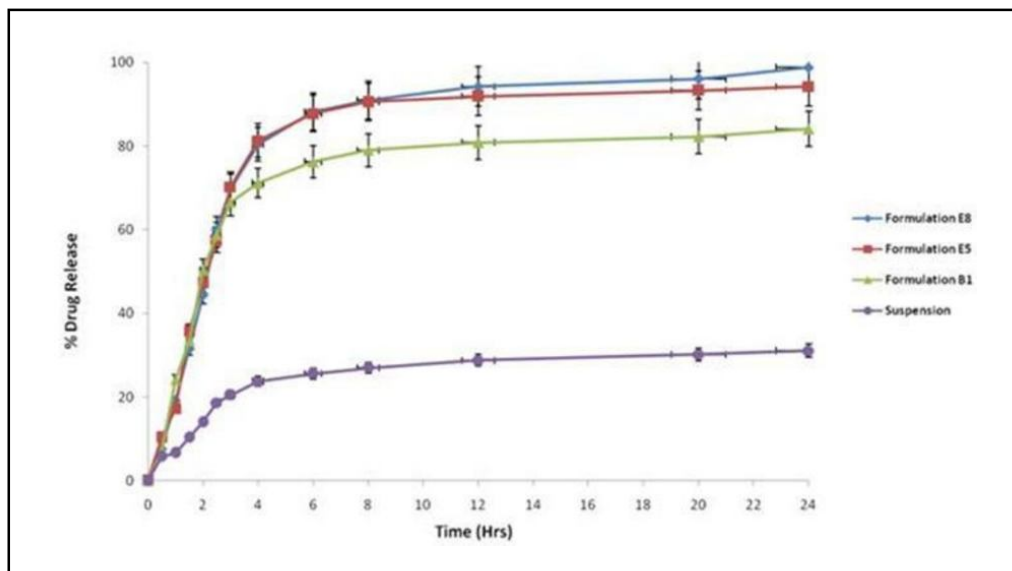


Figure 6: CALN and its comparison with conventional suspension in terms of release of drug.

3.5.5 Experiment to test the stability in accelerated condition

The experiment demonstrated that the optimized CALN did not change in the mean droplet size, PDI, viscosity, zeta potential, % transmittance, and refractive index after storing for 6 months at $40 \pm 2^\circ\text{C}/75 \pm 5\% \text{RH}$. The stability was demonstrated by the absence of phase separation and flocculation. Moreover, an observation was made that as time progressed from 0 to 90 to 180 days the size of the droplets gradually increased and the zeta potential started moving toward zero indicating the movement of droplets towards each other.

3.6 *In vitro* anticancer study

3.6.1 Consequences of CALN and caffeic acid on cells viability of HCT116 cells

According to MTT findings, CALN and caffeic acid exposure to HCT116 cells at different concentrations (0, 10, 20, 30, 40, 50, 75, and 100 ng/ml) and (0, 10, 25, 50, 75, and 100 $\mu\text{g}/\text{ml}$), respectively, caused the death of HCT116 cells in direct proportion manner meaning as the concentration of nanoformulation and caffeic acid increases the cytotoxicity also increases when compared to the corresponding untreated control (Figures 7A and 8A). However, compared to cells exposed to various doses of caffeic acid for the same time period, cells cultivated in CALN showed a greater reduction in cell viability. With an estimated IC_{50} of 74 ng/ml, CALN significantly lowered cell viability in a dose-dependent manner. However, caffeic acid also showed a reduction in cell viability with an IC_{50} of around 120 $\mu\text{g}/\text{ml}$. The active cytotoxic dose of caffeic acid was taken as 20 $\mu\text{g}/\text{ml}$ and 100 $\mu\text{g}/\text{ml}$ while active doses of CALN was taken as 40 ng/ml and 75 ng/ml for further studies.

3.6.2 CALN and caffeic acid altered the cellular morphology in HCT116 cells

The morphological changes noted in HCT116 cells undergoing exposure to caffeic acid 25 $\mu\text{g}/\text{ml}$ and 100 $\mu\text{g}/\text{ml}$ and CALN-40 ng/ml and CALN-75 ng/ml for 24 h are shown in (Figures 7B and 8B). The cells exposed to CALN condition displayed more reduction in cellular morphology and cell adhesion capacity than the cells treated with caffeic acid and their respective untreated control.

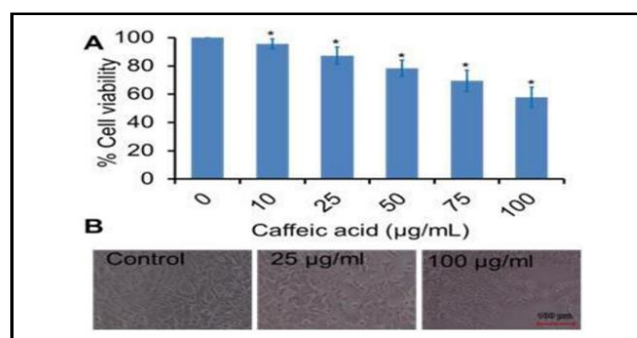


Figure 7: *In vitro* cell viability assay of caffeic acid standard against HCT116 (human colorectal carcinoma) cells, (A) graph showing the percentage of HCT116 (human colorectal cancer) cells that were still viable after being exposed to various doses of caffeic acid standard (0, 10, 25, 50, 75, and 100 $\mu\text{g}/\text{ml}$) and (B) showing morphological changes in HCT116 (human colorectal carcinoma) cells at 25 and 100 $\mu\text{g}/\text{ml}$ concentrations of caffeic acid standard.

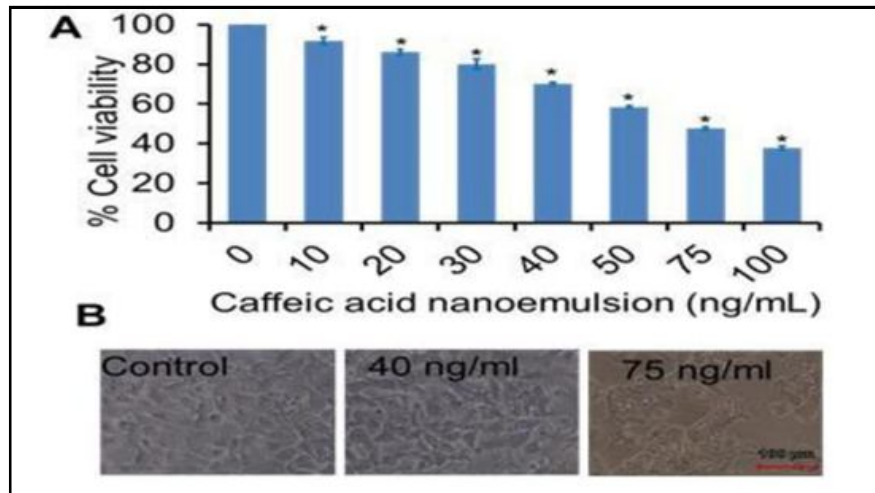


Figure 8: Antiproliferative effect of CALN against HCT116 (human colorectal carcinoma) cells. (A) Graph showing the percentage of HCT116 (human colorectal cancer) cells that were still viable after being exposed to different doses of caffeic acid loaded nanoemulsion (0, 10, 20, 30, 40, 50, 75, and 100 ng/ml) and (B) showing morphological changes in HCT116 (human colorectal carcinoma) cells after treatment with 40 and 75 ng/ml concentrations of caffeic acid loaded nanoemulsion.

3.6.3 DAPI staining to assess the impact of CALN on the chromatin condensation in HCT116 cells

Blebbing of the cell membrane, fragmentation of genomic DNA, and condensation of chromatin are considered to be morphological signs of the apoptotic death process. Two effective dosages of CALN (40 and 75 ng/ml) were utilized to study the apoptotic impact using nuclear fluorescent DAPI. When it binds to AT regions of dsDNA, the blue-fluorescent DNA stain DAPI (42, 6-diamidino-2-phenylindole)

excited by the violet (405 nm) exhibits a 20-fold increase in fluorescence. The photomicrographs exhibited fragmented and condensed nuclei after CALN treatment. The dose-dependent increment in the numbers of apoptotic nuclei and nuclear condensation was observed in the cancerous cells, HCT116, with respect to control cells. In contrast to control cells, cells treated with 75 ng/ml had more apoptotic nuclei and greater nuclear condensation (Figures 9A and 9B).

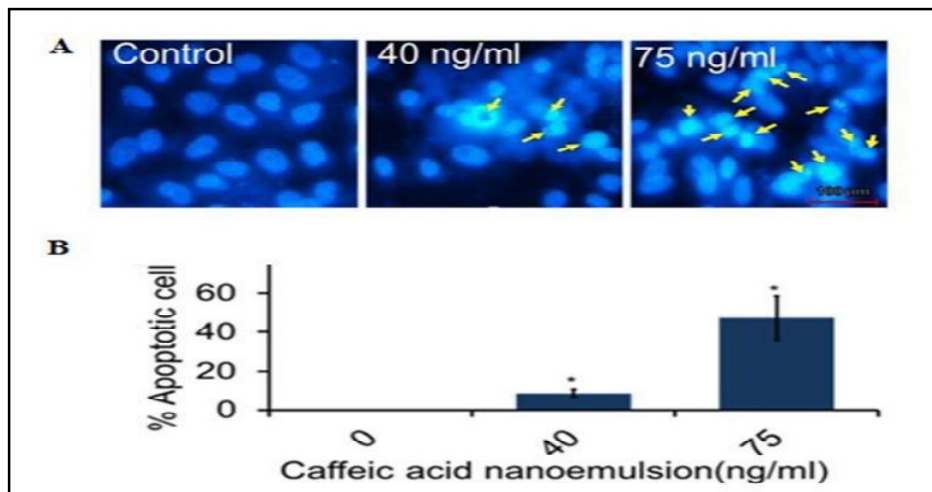


Figure 9: DAPI stained HCT116 (human colorectal cancer) cells exhibited chromatin condensation following treatment with CALN, (A) photomicrographs revealing broken and condensed nuclei, as shown by the arrow were obtained when cells were treated with nanoemulsions containing 40 and 75 ng/ml caffeic acid. A fluorescent phase contrast microscope was used to capture the pictures. Scale bar: 100 μ m and (B) quantitative data is provided as a percentage of apoptotic cells compared to control. To calculate the percentage of apoptotic cells, 100 cells per sample were counted in various areas. Values are reported as the mean \pm standard deviations of three separate studies. $p < 0.05$ as compared to control.

3.6.4 CALN altered the morphology and elevated the ROS generation in HCT116 cells

Figures 10B and 10C show the usual ROS production pictures obtained during the flow cytometric-based DCFH-DA evaluation. When CALN was exposed to HCT116 cells that had been grown in full medium (DMEM with 10% FBS), considerable dose-dependent ROS production was seen. ROS generation has been found much elevated in 75 ng/ml dose. ROS are naturally occurring byproducts of metabolic processes within cells involving oxidation that are essential for cell development,

cell death, cell signaling, and the production of factors that cause inflammation. The main sources for the production of intracellular ROS include microsomes, NOX complexes in cell membranes, endoplasmic reticulum, and peroxisomes. Through the mitochondrial electron-transport system, mitochondria specifically serve as the primary intrinsic source of ROS generation. The levels of ROS were elevated by 7.84% and 37.72% in HCT116 cells when treated with 40 ng/ml and 75 ng/ml of CALN, respectively, compared to the untreated control, suggesting that there was a dose-dependent production of ROS in the cancerous cells (Figures 10A, 10B and 10C).

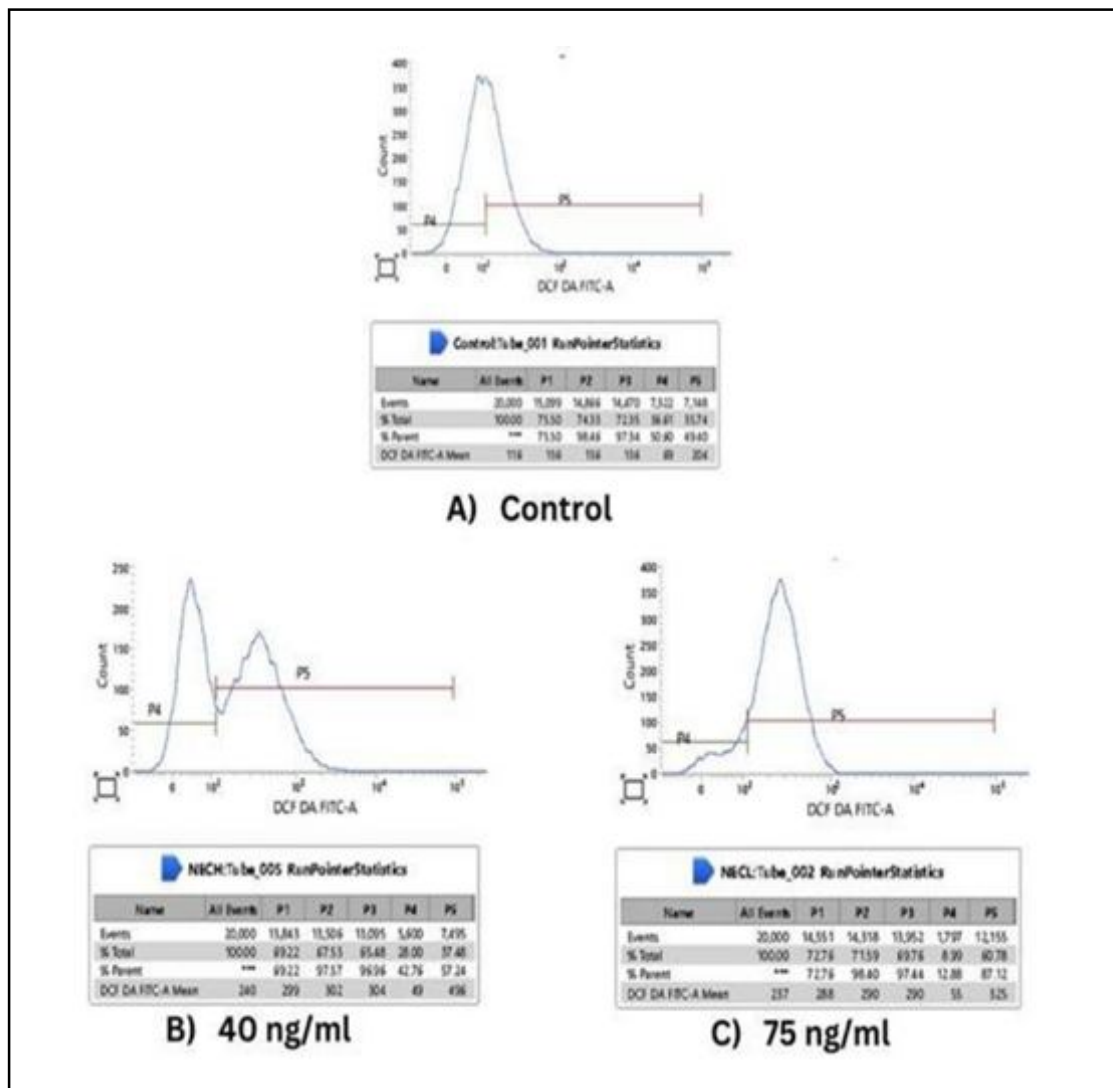


Figure 10: Intracellular ROS generation in HCT116 cells, (A) untreated control, (B) HCT116 cells treated with 40 ng/ml of CALN, and (C) HCT116 cells treated with 75 ng/ml of CALN. The ROS intensity was analyzed through a flow cytometer. The proportion of ROS generation is shown by the fluorescence in the cells.

3.6.5 Analysis of the cell cycle in HCT116 cells and the impact of CALN

The data obtained from the analysis of the cell cycle of HCT116 cells is summarized in Figures 11A, 11B, and 11C. In comparison to the corresponding untreated controls, the data showed that cancerous

cells grown in full medium (DMEM with FBS 10%) and subjected to CALN for 24 h had a severe G2M arrest. The examination of the cell cycle showed that cytotoxicity caused by CALN caused an arrest in the G2M phase. However, there was a considerable increment in the G2M phase exposed to CALN in HCT116 cells at 40 ng/ml (39.21%) and at 75 ng/ml (45.69%).

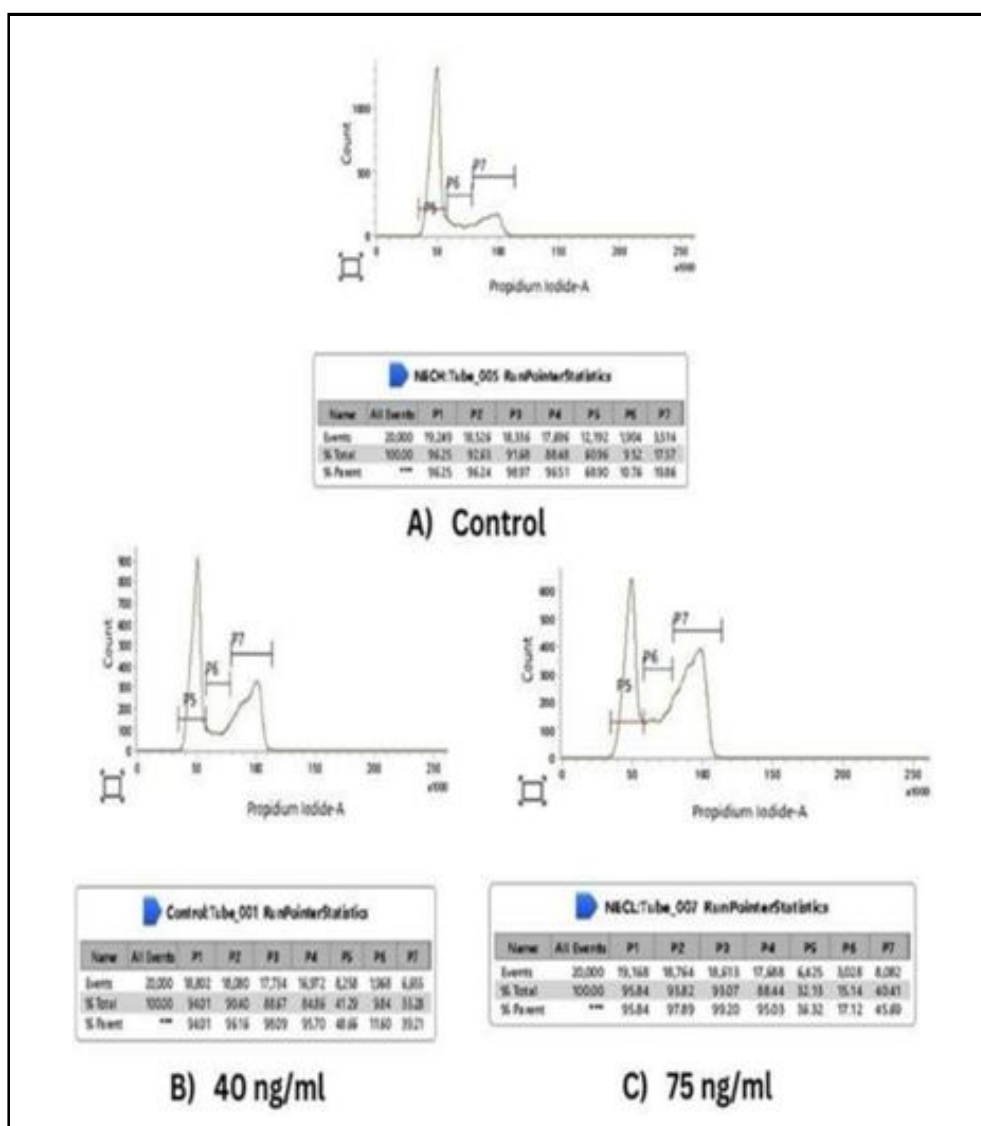


Figure 11: The impact of caffeic acid loaded nanoemulsion on several stages of the cell cycle, (A) untreated control, (B) HCT116 cells were treated with CALN at a concentration of 40 ng/ml, and (C) HCT116 cells were treated with CALN at a dose of 75 ng/ml for 24 h, stained using propidium iodide, and flow cytometry was performed. Photomicrographs demonstrate the phase distribution of the cell density at various stages of the cell cycle.

4. Discussion

This study aimed to develop and investigate the potential of caffeic acid loaded nanoemulsions (CALN) as a potential anticancer nanoformulation. The research involved optimizing the composition of nanoemulsion by carefully adjusting the ratios of critical components, including the oil phase, surfactants, co-surfactants, and the aqueous phase. The findings indicated that a S_{mix} ratio of 2:1 (comprising Triton X100 as the surfactant and propylene glycol as the co-surfactant) with distilled water as the aqueous phase provided the best results. To this optimized nanoemulsion caffeic acid was added to produce CALN which demonstrated remarkable stability over six months under accelerated storage conditions. Characterization of CALN revealed that the optimized formulation (E8) had the

smallest droplet size, a crucial feature for efficient drug delivery systems. It also exhibited rapid drug release kinetics, making it a promising option for effective drug delivery. The consistent droplet size distribution within the CALN implied that the selected formulation could maintain its stability over time. *In vitro* experiments involving human colorectal carcinoma cells (HCT116) provided insights into CALN's potential as an anticancer agent. Both caffeic acid and CALN exhibited dose-dependent cytotoxicity, with CALN consistently outperforming caffeic acid in reducing cell viability. CALN induced significant changes in cellular morphology, leading to reduced cell adhesion and viability, reinforcing its potential as an anticancer agent. CALN also triggered apoptosis, evident through nuclear condensation and fragmentation, indicating its capacity to induce cell death in cancer cells. Additionally, CALN increased the generation of ROS

(reactive oxygen species) in HCT116 cells. Elevated ROS levels can contribute to oxidative stress and apoptosis in cancer cells, suggesting a potential mechanism for CALN's anticancer effects. In summary, the optimized CALN displayed promising attributes in terms of stability, drug release, and anticancer potential against *in vitro* colorectal cancer model.

5. Conclusion

An optimized CALN was developed using the oil phase (sefsol 218), S_{mix} ratio 2:1 (surfactant as triton X100 and co-surfactant as propylene glycol), and distilled water as aqueous phase whose concentration was 12% v/v, 28% v/v and 60% v/v, respectively. The prepared CALN were investigated in terms of size of the droplet, PDI, refractive index, zeta potential, % transmittance, and viscosity, and formulation E8 was found to be the best amongst others and its droplet size result coincided with the size of droplets produced by TEM. Moreover, the drug release of formulation E8 in 24 h was 98.81% which again was the highest among other prepared CALN. Findings from the stability test showed that the optimised CALN was stable for six months storage term at $40 \pm 2^\circ\text{C}/75 \pm 5\%$ RH since the formulations did not cream, crack, flocculate, or separate into phases. The *in vitro* study assessed CALN and caffeic acid's effects on HCT116 cells. Although, CALN showed greater diminished cell viability, both caffeic acid and CALN demonstrated dose-dependent cytotoxicity. In HCT116 cells, treatment with CALN resulted in altered cellular shape, increased ROS production, and triggered G2M phase arrest. Additionally, CALN induced nuclear condensation and fragmentation, are signs of apoptosis induction. These findings point to the potential of CALN as an effective anticancer formulation, but further *in vivo* research is required to confirm both its efficacy and safety.

Acknowledgements

Authors are thankful to the Honorable Chancellor and Vice Chancellor, Integral University for providing necessary facilities and suggestions regarding improvement of the manuscript and special thanks to Dean, Research and Development committee for providing manuscript communication number IU/R&D/2023-MCN0001999 for publishing in the journal.

Conflict of interest

The authors declare no conflicts of interest relevant to this article.

References

Agunloye, O. M.; Oboh, G.; Ademiluyi, A. O.; Ademosun, A. O.; Akindahunsi, A. A.; Oyagbemi, A. A.; Omobowale, T. O.; Ajibade, T. O. and Adedapo, A. A. (2019). Cardioprotective and antioxidant properties of caffeic acid and chlorogenic acid: Mechanistic role of angiotensin converting enzyme, cholinesterase and arginase activities in cyclosporine induced hypertensive rats. *Biomedicine and Pharmacotherapy*, 109:450-458. <https://doi.org/10.1016/j.biopha.2018.10.044>, PubMed:30399581

Ahmad, U.; Akhtar, J.; Singh, S. P.; Ahmad, F. J. and Siddiqui, S. (2018). Silymarin nanoemulsion against human hepatocellular carcinoma: Development and optimization. *Artificial Cells, Nanomedicine, and Biotechnology*, 46(2):231-241. <https://doi.org/10.1080/21691401.2017.1324465>, PubMed: 28503949.

Akhtar, J. (2015). Novel oral nanoemulsion based drug delivery system of antidiabetic Drug [Dissertation]. Integral University.

Akhtar, J.; Siddiqui, H. H.; Badruddeen, S.; Fareed, S. and Aqil, M. (2014). Nanoemulsion as a carrier for efficient delivery of metformin. *Current Drug Delivery*, 11(2):243-252. <https://doi.org/10.2174/156720181102140411160817>, PubMed: 24410150

Akhtar, J.; Siddiqui, H. H.; Fareed, S.; Badruddeen, K. M.; Khalid, M. and Aqil, M. (2016). Nanoemulsion: For improved oral delivery of repaglinide. *Drug Delivery*, 23(6):2026-2034. <https://doi.org/10.3109/10717544.2015.1077290>, PubMed: 27187792

Aungst, B. J. (1993). Novel formulation strategies for improving oral bioavailability of drugs with poor membrane permeation or presystemic metabolism. *Journal of Pharmaceutical Sciences*, 82(10):979-987. <https://doi.org/10.1002/jps.2600821008>, PubMed: 8254497

Aungst, B. J.; Nguyen, N.; Rogers, N. J.; Rowe, S.; Hussain, M.; Shum, L. and White, S. (1994). Improved oral bioavailability of an HIV protease inhibitor using gelucire 44/14 and labrasol vehicles. *BT Gattefosse*, 87:49-54.

Baker, D. D.; Chu, M.; Oza, U. and Rajgarhia, V. (2007). The value of natural products to future pharmaceutical discovery. *Natural Product Reports*, 24(6):1225-1244. <https://doi.org/10.1039/b602241n>, PubMed: 18033577

Bispo, V. S.; Dantas, L. S.; Chaves, A. B.; Pinto, I. F. D.; Silva, R. P. D.; Otsuka, F. A. M.; Santos, R. B.; Santos, A. C.; Trindade, D. J. and Matos, H. R. (2017). Reduction of the DNA damages, hepatoprotective effect and antioxidant potential of the coconut water, ascorbic and caffeic acids in oxidative stress mediated by ethanol. *Anais da Academia Brasileira de Ciencias*, 89(2):1095-1109. <https://doi.org/10.1590/0001-3765201720160581>, PubMed: 28513780

Burcham, D. L.; Maurin, M. B.; Hausner, E. A. and Huang, S. M. (1997). Improved oral bioavailability of the hypocholesterolemic DMP 565 in dogs following oral dosing in oil and glycol solutions. *Biopharmaceutics and Drug Disposition*, 18(8):737-742. [https://doi.org/10.1002/\(sici\)1099-081x\(199711\)18:8<737::aid-bdd59>3.0.co;2-9](https://doi.org/10.1002/(sici)1099-081x(199711)18:8<737::aid-bdd59>3.0.co;2-9), PubMed: 9373730

Chang, W. C.; Hsieh, C. H.; Hsiao, M. W.; Lin, W. C.; Hung, Y. C. and Ye, J. C. (2010). Caffeic acid induces apoptosis in human cervical cancer cells through the mitochondrial pathway. *Taiwanese Journal of Obstetrics and Gynecology*, 49(4):419-424. [https://doi.org/10.1016/S1028-4559\(10\)60092-7](https://doi.org/10.1016/S1028-4559(10)60092-7), PubMed: 21199742

Deka, Naba J.; Nath, R.; Tamuly, S.; Hazorika, M.; Pegu, S. R. and Deka, S. M. (2021). Green synthesis and characterization of silver nanoparticles using leaves extract of neem (*Azadirachta indica* L.) and assessment of its *in vitro* antioxidant and antibacterial activity. *Ann. Phytomed.*, 10(1):171-177. <http://doi.org/10.21276/ap.2021.10.1.17>

Dixit, S. and Ali, H. (2010). Anticancer activity of medicinal plant extract: A review. *Journal of Chemical Sciences*, 1(1):79-85.

Genaro-Mattos, T. C.; Maurício, Â. Q.; Rettori, D.; Alonso, A. and Hermes-Lima, M. (2015). Antioxidant activity of caffeic acid against iron-induced free radical generation: A chemical approach. *PLOS ONE*, 10(6):e0129963. <https://doi.org/10.1371/journal.pone.0129963>, PubMed: 26098639

- Gu, W.; Yang, Y.; Zhang, C.; Zhang, Y.; Chen, L.; Shen, J.; Li, G.; Li, Z.; Li, L.; Li, Y. and Dong, H. (2016). Caffeic acid attenuates the angiogenic function of hepatocellular carcinoma cells *via* reduction in JNK-1-mediated HIF-1 α stabilization in hypoxia. *RSC Advances*, **6**(86):82774-82782. <https://doi.org/10.1039/C6RA07703J>
- Imad Uddin, M. D. and Veeresh, B. (2020). Systematic review on screening the role of chemosensitizer or synergistic drug and doxorubicin as dual drug loaded nanoparticle in overcoming multidrug resistant breast cancer. *Ann. Phytomed.*, **9**(2):113-124. <http://dx.doi.org/10.21276/ap.2020.9.2.9>
- Imad Uddin, M. D.; Srikar, P. V. R.; Karunya, Y. P.; Chakraborty, R and R. Deepika. (2020). *Synthe.*, **23**:462369
- Mehnert, W. and Mader, K. (2012). Solid lipid nanoparticles: Production, characterization and applications. *Advanced Drug Delivery Reviews*, **64**:83-101.
- Myers, R. A. and Stella, V. J. (1992). Systemic bioavailability of penclomedine (NSC-338720) from oil-in-water emulsions administered intraduodenally to rats. *International Journal of Pharmaceutics*, **78**(1-3): 217-226. [https://doi.org/10.1016/0378-5173\(92\)90374-B](https://doi.org/10.1016/0378-5173(92)90374-B)
- Nagaoka, T.; Banskota, A. H.; Tezuka, Y.; Saiki, I. and Kadota, S. (2002). Selective antiproliferative activity of caffeic acid phenethyl ester analogues on highly liver-metastatic murine colon 26-L5 carcinoma cell line. *Bioorganic and Medicinal Chemistry*, **10**(10):3351-3359. [https://doi.org/10.1016/S0968-0896\(02\)00138-4](https://doi.org/10.1016/S0968-0896(02)00138-4), PubMed: 12150882
- Ozturk, G.; Ginis, Z.; Akyol, S.; Erden, G.; Gurel, A. and Akyol, O. (2012). The anticancer mechanism of caffeic acid phenethyl ester (CAPE): Review of melanomas, lung and prostate cancers. *European Review for Medical and Pharmacological Sciences*, **16**(15):2064-2068. PubMed: 23280020
- Palin, K. J.; Phillips, A. J. and Ning, A. (1986). The oral absorption of cefoxitin from oil and emulsion vehicles in rats. *International Journal of Pharmaceutics*, **33**(1-3):99-104. [https://doi.org/10.1016/0378-5173\(86\)90043-8](https://doi.org/10.1016/0378-5173(86)90043-8)
- Parveen, R.; Ahmad, S.; Baboota, S.; Ali, J. and Alka, A. (2010). Stability indicating HPTLC method for quantitative estimation of silybin in bulk drug and pharmaceutical dosage form. *Biomedical Chromatography*, **24**(6):639-647. <https://doi.org/10.1002/bmc.1340>, PubMed: 19816854
- Prakash, O. M.; Kumar, A.; Kumar, P. and Ajeet, A. (2013). Anticancer potential of plants and natural products: A review. *American Journal of Pharmacological Sciences*, **1**(6):104-115. <https://doi.org/10.12691/ajps-1-6-1>
- Rodrigues, J. L.; Araújo, R. G.; Prather, K. L.; Kluskens, L. D. and Rodrigues, L. R. (2015). Heterologous production of caffeic acid from tyrosine in *Escherichia coli*. *Enzyme and Microbial Technology*, **71**:36-44. <https://doi.org/10.1016/j.enzmictec.2015.01.001>, PubMed: 25765308
- Saroha, A.; Kotiyal, A. and Rupesh, R. (2023). Nanoemulsion: A futuristic approach to disease elimination for food safety. *Ann. Phytomed.*, an International Journal, **12**(1):180-186. <https://doi.org/10.54085/ap.2023.12.1.50>
- Schwendener, R. A. and Schott, H. (1996). Lipophilic 1- β -D-arabinofuranosyl cytosine derivatives in liposomal formulations for oral and parenteral antileukemic therapy in the murine L1210 leukemia model. *Journal of Cancer Research and Clinical Oncology*, **122**(12):723-726. <https://doi.org/10.1007/BF01209119>, PubMed: 8954169
- Serajuddin, A. T. (1999). Solid dispersion of poorly water soluble drugs: Early promises, subsequent problems, and recent breakthroughs. *Journal of Pharmaceutical Sciences*, **88**(10):1058-1066. <https://doi.org/10.1021/js9804031>, PubMed: 10514356
- Serajuddin, A. T.; Sheen, P. C.; Mufson, D.; Bernstein, D. F. and Augustine, M. A. (1988). Effect of vehicle amphiphilicity on the dissolution and bioavailability of a poorly water soluble drug from solid dispersions. *Journal of Pharmaceutical Sciences*, **77**(5):414-417. <https://doi.org/10.1002/jps.2600770512>, PubMed: 3411464
- Shafiq, S.; Shakeel, F.; Talegaonkar, S.; Ahmad, F. J.; Khar, R. K. and Ali, M. (2007). Development and bioavailability assessment of ramipril nanoemulsion formulation. *European Journal of Pharmaceutics and Biopharmaceutics*, **66**(2):227-243. <https://doi.org/10.1016/j.ejpb.2006.10.014>, PubMed: 17127045
- Shafiq-un-Nabi, S.; Shakeel, F.; Talegaonkar, S.; Ali, J.; Baboota, S.; Ahuja, A.; Khar, R. K. and Ali, M. (2007). Formulation development and optimization using nanoemulsion technique: A technical note. *AAPS PharmSciTech*, **8**(2):Article 28. <https://doi.org/10.1208/pt0802028>, PubMed: 17622106
- Shi, J.; Votruba, A. R.; Farokhzad, O. C. and Langer, R. (2010). Nanotechnology in drug delivery and tissue engineering: From discovery to applications. *Nano Letters*, **10**(9):3223-3230. <https://doi.org/10.1021/nl102184c>, PubMed: 20726522
- Siddiqui, S. and Arshad, M. (2014). Osteogenic potential of Punica granatum through matrix mineralization, cell cycle progression and runx2 gene expression in primary rat osteoblasts. *DARU: Journal of Pharmaceutical Sciences*, **22**:1-8.
- Silva, T.; Oliveira, C. and Borges, F. (2014). Caffeic acid derivatives, analogs and applications: A patent review. *Expert Opinion on Therapeutic Patents*, **24**(11):1257-1270. <https://doi.org/10.1517/13543776.2014.959492>, PubMed: 25284760
- Singh, S.; Kushwaha, P. and Gupta, S. (2022). Development and evaluation of thermoresponsive in situ nanoemulgel of myricetin for diabetic retinopathy. *Ann. Phytomed.*, **11**(1):320-326. <http://dx.doi.org/10.54085/ap.2022.11.1.33>
- Toguchi, H.; OGAWA, Y.; IGA, K. and Shimamoto, T. (1990). Effects of physiological factors on the bioavailability of ethyl 2-chloro-3-[4-(2-methyl-2-phenylpropyloxy)phenyl] propionate in an emulsion in rats. *Chemical and Pharmaceutical Bulletin*, **38**(10):2801-2804.
- Tosovic, J. (2017). Spectroscopic features of caffeic acid: Theoretical study. *Kragujevac Journal of Science*, **39**:99-108.
- Verma, R. P. and Hansch, C. (2004). An approach towards the quantitative structure activity relationships of caffeic acid and its derivatives. *Chem. Bio. Chem.*, **5**(9):1188-1195. <https://doi.org/10.1002/cbic.200400094>, PubMed: 15368569

- Wagner, V.; Dullaart, A.; Bock, A. K. and Zweck, A. (2006). The emerging nanomedicine landscape. *Nature Biotechnology*, **24**(10):1211-1217. <https://doi.org/10.1038/nbt1006-1211>, PubMed: 17033654
- Wang, S. J.; Zeng, J.; Yang, B. K. and Zhong, Y. M. (2014). Bioavailability of caffeic acid in rats and its absorption properties in the Caco-2 cell model. *Pharmaceutical Biology*, **52**(9):1150-1157. <https://doi.org/10.3109/13880209.2013.879906>, PubMed: 24635458
- Won, C.; Lee, C. S.; Lee, J. K.; Kim, T. J.; Lee, K. H.; Yang, Y. M.; Kim, Y. N.; Ye, S. K. and Chung, M. H. (2010). CADPE suppresses cyclin D1 expression in hepatocellular carcinoma by blocking IL-6-induced STAT3 activation. *Anticancer Research*, **30**(2):481-488. PubMed: 20332458
- Wu, W.; Wang, Y. and Que, L. (2006). Enhanced bioavailability of silymarin by self-microemulsifying drug delivery system. *European Journal of Pharmaceutics and Biopharmaceutics*, **63**(3):288-294. <https://doi.org/10.1016/j.ejpb.2005.12.005>, PubMed: 16527467
- Xie, J.; Yang, F.; Zhang, M.; Lam, C.; Qiao, Y.; Xiao, J.; Zhang, D.; Ge, Y.; Fu, L. and Xie, D. (2017). Antiproliferative activity and SARs of caffeic acid esters with mono-substituted phenylethanols moiety. *Bioorganic and Medicinal Chemistry Letters*, **27**(2):131-134. <https://doi.org/10.1016/j.bmcl.2016.12.007>, PubMed: 27979593
- Yang, S. Y.; Hong, C. O.; Lee, G. P.; Kim, C. T. and Lee, K. W. (2013). The hepatoprotection of caffeic acid and rosmarinic acid, major compounds of perilla frutescens, against t-BHP-induced oxidative liver damage. *Food and Chemical Toxicology*, **55**:92-99. <https://doi.org/10.1016/j.fct.2012.12.042>, PubMed: 23306788
- Zhang, P.; Ye, H.; Min, T. and Zhang, C. (2008). Water soluble poly(ethylene glycol) prodrug of silybin: Design, synthesis, and characterization. *Journal of Applied Polymer Science*, **107**(5):3230-3235. <https://doi.org/10.1002/app.27450>
- Citation** Asad Ali, Usama Ahmad, Juber Akhtar, Badruddeen, Khursheed Ahmad, Shivbrat Upadhyay, Sahabjada Siddiqui, Rumana Ahmad, Puneet Khare, Mohd Muazzam Khan and Afroz Jahan (2023). Exploring the anticancer potential of caffeic acid nanoemulsion: ROS induced apoptosis and cell cycle arrest in HCT116 colorectal cancer cells. *Ann. Phytomed.*, **12**(2):463-478. <http://dx.doi.org/10.54085/ap.2023.12.2.57>.